Oxidation of Metals (2019) 92:303–313
https://doi.org/10.1007/s11085-019-09928-8

ORIGINAL PAPER

Effects of Hf, Y, and Zr on Alumina Scale Growth on NiAlCr and NiAlPt Alloys

DongEung Kim[1,3] · Shun-Li Shang[1] · Zhuoqun Li[2] · Brian Gleeson[2] · Zi-Kui Liu[1]

Received: 7 April 2015 / Revised: 7 May 2017 / Published online: 23 July 2019

Abstract

The effects of Hf, Y, and Zr additions on the growth of a thermally grown alumina scale formed on NiAlCr and NiAlPt alloys were investigated. Isothermal and thermal cycling oxidation experiments were carried out at 1150 °C, and cross sections of the oxidized samples were characterized using scanning electron microscopy. It was observed that single doping as well as co-doping of Hf, Y, and Zr reduces the rate of alumina scale growth on NiAlCr and NiAlPt alloys, with Hf showing a more significant effect than Y or Zr. The following possible contributing factors to these observations were assessed: (1) the ionic size of the minor alloying elements and (2) the bond strength between the doping elements and oxygen in the oxide grain boundaries in terms of formation and melting enthalpies of oxides. It was concluded that the bond strength between the doping elements and oxygen within the oxide grain boundaries plays an important role in retarding the alumina scale growth.

Keywords Alumina · Reactive elements · Scale growth

Introduction

Thermal barrier coating (TBC) systems are widely used in gas turbine engines to protect metal components such as turbine blades from the high-temperature engine environment. A TBC system primarily consists of four layers made of different materials with specific properties and functions: (1) the ceramic topcoat of Y_2O_3-stablilzed ZrO_2 that provides the thermal insulation [1]; (2) the thermally

✉ DongEung Kim
canon@kitech.re.kr

[1] Department of Materials Science and Engineering, The Pennsylvania State University, University Park, PA 16802, USA

[2] Department of Mechanical Engineering and Materials Science, University of Pittsburgh, Pittsburgh, PA 15261, USA

[3] Korea Institute of Industrial Technology (KITECH), Gaetbeol-ro 156, Yeonsu-gu, Incheon 21999, Republic of Korea

grown oxide (TGO) of α-Al_2O_3 that is inevitably formed between the ceramic topcoat and the bond coat [2]; (3) the bond coat that is a metallic layer used to provide oxidation resistance and to connect the ceramic topcoat to the substrate; and (4) the Ni-base superalloy substrate [3].

Since the formation of a TGO layer is both inevitable and essential, the bond coat is thus engineered to form a uniform and continuous α-Al_2O_3 layer for extended protection [4]. The growth of α-Al_2O_3 scales is controlled by the solid-state transport of both oxygen and aluminum [5]. Furthermore, oxygen tracer studies of α-Al_2O_3 growth on NiAlCr + Zr alloys at 1100 °C have shown that outward transport of Al^{3+} cation has a small contribution to overall scale growth, while inward grain boundary transport of oxygen anions is dominant [6]. Earlier studies [7, 8] similarly concluded that the scale growth on FeAlCr and NiAlCr alloys doped with reactive elements (e.g., Hf, Y, Zr) is primarily dictated by inward oxygen diffusion, with the scale grain boundaries providing the main transport paths. In apparent contradiction, the two-stage oxidation studies [9–11] show that a considerable amount of Al transport can occur during the relatively early stages of scale growth. This is largely due to the formation of metastable Al_2O_3 prior to the establishment of the more stable α-Al_2O_3. It is generally inferred that the metastable γ and θ polymorphs of Al_2O_3 grow primarily by the outward transport of Al^{3+} ions [5].

In the recent works of Heuer et al. [12–14], a disconnection mechanism of grain boundary diffusion was proposed to rationalize past diffusion studies associated with α-Al_2O_3. They also showed that dopant segregation to the α-Al_2O_3 grain boundaries changes the band structure by significantly reducing the near-band edge states, which in turn reduces the propensity for Al ionization. This has the effect of significantly decreasing the Al^{3+} flux in the scale relative to that of O^{2-}. They postulated that the charge compensation reaction when reactive element (RE), especially Hf, segregates to the Al_2O_3 grain boundaries may affect grain boundary diffusion of Al by reducing the electronic conductivity of the grain boundary. It is postulated in this study that, since diffusion involves the breaking of metal–oxygen bonds, the charge compensation reaction may manifest through the bond energy difference between Al–O and RE–O bonds, which is closely related to their formation enthalpy.

The present work examines experimentally the influence of reactive elements Hf, Y, and Zr on the growth rates of α-Al_2O_3 scales formed on NiAlCr and NiAlPt alloys. The observations are analyzed in terms of the size of doping elements and the bonding strength between doping elements and oxygen. We aim to correlate the formation and melting enthalpies of oxides with their bonding strength and provide insights into their relative effectiveness in retarding the scale growth.

Experimental Procedures

Cr and Pt-modified Ni_3Al-base alloys with nominal compositions Ni–20Al–5Cr and Ni–22Al–30Pt (in at.% throughout the text unless specified otherwise) with or without the additions of reactive elements Hf, Y, and Zr were prepared by argon arc melting of high-purity constituents (~99.99% pure). To ensure homogenization and equilibration, all alloys were annealed at 1150 °C for 48 h in a flowing argon

atmosphere and then quenched in water to retain their high-temperature structure. These alloys were then cut into coupon samples and polished to a 600-grit finish. The equilibrated alloy samples were first analyzed using X-ray diffraction (XRD) for phase identification and then prepared for metallographic analyses by cold mounting them in an epoxy resin followed by polishing to a 0.5-μm finish.

Isothermal and cyclic oxidation tests were carried out at 1150 °C in air using an open, vertical furnace equipped with a timer-controlled sample elevation unit (see details in Ref. [15]). In the case of isothermal oxidation testing, weight change was monitored continuously via thermogravimetric analysis (TGA). The weight change of the TGA-tested samples was checked at the completion of a given test by measuring the sample mass using an analytical balance. In the case of cyclic oxidation testing, each thermal cycle consisted of 1 h at 1150 °C followed by 15 min at room temperature with the sample weight measured intermittently using an analytical balance. At the end of a given test, the oxidized samples were prepared using standard metallographic procedures and then examined using a scanning electron microscope (SEM).

Results and Discussions

Figure 1 shows measured isothermal oxidation kinetics in air at 1150 °C of Ni–20Al–5Cr-base alloys with Y or Hf added separately (i.e., single doped) or Y and Hf added together (i.e., co-doped). The doping levels of Hf and Y are 0.1 and 0.05 at.%, respectively. At these levels, whether single doped or co-doped, the oxidation kinetics are always slower than those without any RE additions. In terms of reducing the oxidation kinetics, the dopants and their contents rank as follows in descending order (i.e., from the most effective to least): 0.05–0.1 Hf, 0.1 Hf + 0.05

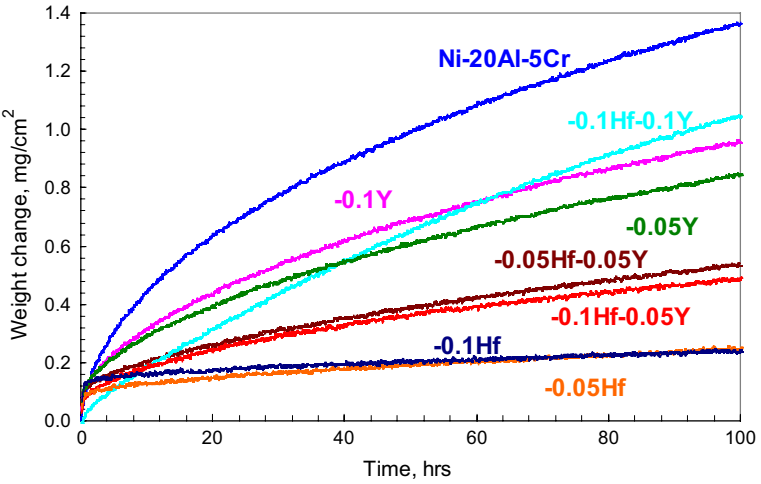

Fig. 1 Weight changes of reactive element-doped Ni–20Al–5Cr (at.%) alloys as a function of isothermal exposure time at 1150 °C in air

Y, 0.05 Hf + 0.05 Y, 0.05 Y, 0.1 Y, and 0.1 Hf + 0.1 Y. Cross-sectional SEM images of the selected alloys from the isothermal oxidation test at 1150 °C are shown in Fig. 2. The alumina scales on the alloys with Hf and/or Y are seen to be significantly thinner, which is in accordance with the weight change measurements in Fig. 1. Figure 3 compares the cyclic oxidation kinetics of Ni–22Al–30Pt alloys with and without the addition of Hf or Zr at 1150 °C in air. It is observed that the addition of Hf or Zr significantly decreases the weight gain and, therefore, slows the rate of TGO scale growth, with the effect of Hf being the greatest.

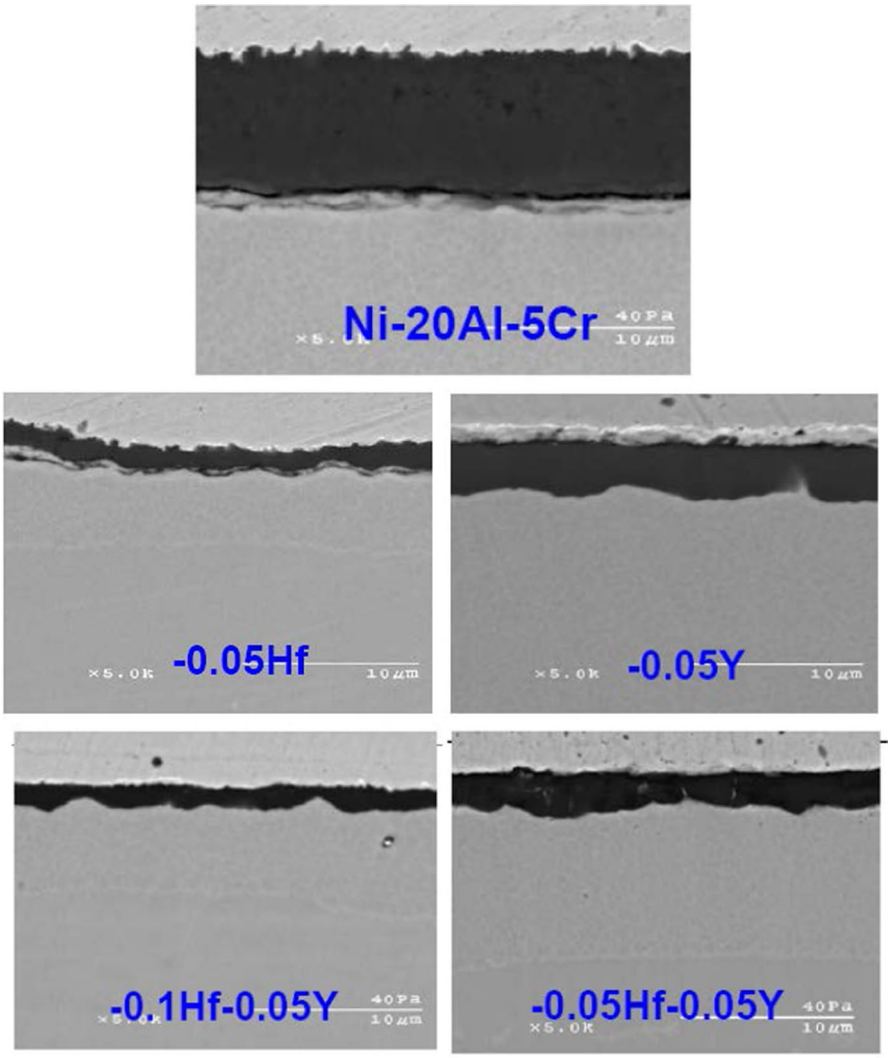

Fig. 2 Cross-sectional images of Ni–20Al–5Cr (at.%) alloys with and without additions of reactive elements at 1150 °C

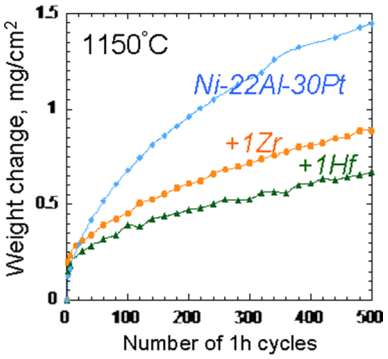

Fig. 3 Comparison of cyclic oxidation kinetics of Ni–22Al–30Pt (at.%) alloys, with and without the addition of Hf and Zr 1150 °C in air

In the following discussion, the observed effects of doping concentration and co-doping effects are discussed in terms of ionic size, bonding strength between doping elements and oxygen, and the oxide-scale microstructure. It is important to realize that the RE doping concentrations reported are in the alloy, not in the scale, and that the REs in the TGO grain boundaries are supplied from the alloy.

Size Effect

The tendency of a cationic impurity segregating to Al_2O_3 grain boundaries is generally explained by the difference in ionic size mismatch between that segregating cation and Al^{3+} [16]. It has been reported that Y^{3+} or Zr^{4+}, both larger than Al^{3+}, shows a strong tendency to segregate to Al_2O_3 grain boundaries [17]. In addition, it has been reported that Y^{3+} and La^{3+} segregate to Al_2O_3 grain boundaries and reduce the tensile creep rate of Al_2O_3 [18], while in the cases of Cr^{3+} and Fe^{3+}, which have similar ionic radii to Al^{3+}, doping does not result in improvement in creep properties [19]. It is also found that Y doping can suppress the grain boundary diffusion [20] and consequently reduce the growth rate of Al_2O_3 scales [21, 22].

The effect of reactive elements with a larger ionic size than Al^{3+} in reducing the TGO growth rate is commonly referred as the so-called site blocking effect [19]. It is known that the ionic radius varies with the coordination numbers [23]. Al in Al_2O_3 and Y in Y_2O_3 have six nearest neighbors of oxygen and Zr in ZrO_2 has at least seven nearest neighbors of oxygen, while Hf in HfO_2 is coordinated with eight oxygen in its monoclinic ground state. However, in the grain boundary, the cation-oxygen coordination numbers have been found to reduce to 4, 4.2, 5, and 5 for the oxides of Al, Y, Hf, and Zr, respectively, based on both experimental measurements [24] and theoretical analysis [25]. Since Y, Hf, and Zr have higher coordination numbers than Al, they reduce the available sites for Al to diffuse through, which ostensibly contributes to the interpretation of a "site blocking" effect.

The calculated ionic radii of Y, Hf, Zr, and Al cations in the respective oxide grain boundaries according to the above-stated coordination numbers are summarized in Table 1. These calculated radii are based on data from Shannon [23, 26], who derived approximately linear relationships between ionic volume and unit-cell volume in oxides and fluorides from numerous experimentally measured

Table 1 Comparison of coordination number in grain boundary (CN-GB), cation radius (Å), melting temperature (°C), equilibrium volume (A^3/atom), bulk modulus (GPa), enthalpy of formation ($\Delta_f H$), and enthalpy of melting ($\Delta_m H$) (kJ/mol of metallic atoms) of various oxides

	CN-GB	Cation radius[c]	T_m^i	Equilibrium volume		Bulk modulus		$\Delta_f H$	$\Delta_m H$
				Exp	Calc	Exp	Calc	Calc[i]	Calc[i]
HfO_2	5[a]	~0.65	2800	10.92[e]	11.00[e], 10.83[e]	–	248[e], 251[f]	−1116	126
ZrO_2	5 ± 0.5[b]	~0.66	2710	10.99[e]	11.15[e]	194–254[e]	237[e]	−1100	111
					10.75[e]		221[e]		
					10.90[e]		268[e]		
					10.53[e]		310[e]		
					10.62[e]		222[e]		
							157[f]		
Y_2O_3	4.2 ± 0.5[b]	~0.79	2439	14.90[g]	14.16[g]	150[g]	180[g]	−953	68
	5[a]	~0.84				170[g]	182[g]		
						57–177[g]	183[g]		
Al_2O_3	4[a,b]	0.39	2054	8.49[h]	8.35[h]	254[h]	232[h]	−838	56
					8.75[h]		259[h]		

[a]Reference [25]

[b]Reference [24]

[c]Shannon effective ionic radii, Reference [23]

[d]Reference [45, 46]

[e]Reference [33]

[f]Reference [47]

[g]Reference [48]

[h]Reference [49]

[i]SGTE Substance database, Reference [32]

inter-atomic distances. The Hf^{4+} radius with a coordination number equal to five is interpolated from available radii with coordination numbers of 4, 6, 7, and 8, since the coordination number and the ionic radius show a linear relationship for Hf [23]. As shown in Table 1, the radii of Y^{3+}, Hf^{4+} and Zr^{4+} are all larger than that of Al^{3+} for their respective coordination numbers in the grain boundary.

However, Fig. 1 shows that the addition of Hf (0.1 and 0.05 at.%) reduces the weight gain much more than the same amount of Y, even though the size of Y^{3+} is much larger than that of Hf^{4+}. It is also observed in Fig. 3 that the addition of 1 at.% of Hf has a more significant effect than the addition of 1 at.% Zr in decreasing the weight gain during oxidation, even though the radius of Hf^{4+} is slightly smaller. Therefore, the ionic size is not a reliable factor in determining the influence of reactive elements on the TGO growth. As mentioned earlier, Heuer et al. [27] suggested that the REs may affect the oxidation behavior not by a geometric effect but rather by reducing Al ionization by modifying the grain boundary donor and acceptor states. When RE is added, the electronic structure of Al_2O_3 is changed, resulting in reducing the tendency for Al to be ionized as RE–O bonding is preferred. In the

following section, we will discuss the effect of ionization on the scale growth in the grain boundary in terms of breaking bonds between the cation and oxygen.

Cation-O^{2-} Bonding Strength

The diffusion of Al^{3+} and O^{2-} in the grain boundary involves the breaking and forming of Al-O bonds. This is true even if the diffusion is by a disconnection mechanism. The bond strength must thus be important and may be considered in terms of bulk modulus [28, 29] and enthalpy of formation [30], both of which will be discussed in the following along with the enthalpy of melting and bond length.

The bulk modulus is widely considered to be an indicator of bonding strength [28, 29]. However, it is known that the bulk modulus is inversely proportional to volume [31], and so any comparison of bulk modulus needs to be made with similar volumes of compounds. Among the oxides considered in the present work, Y_2O_3 has the largest volume, resulting in the lowest bulk modulus (see Table 1). In contrast, the bulk modulus of Al_2O_3 is the highest due to its smallest equilibrium volume. On the other hand, the atomic volumes of HfO_2 and ZrO_2 are close to each other and between those of Y_2O_3 and Al_2O_3. The significantly higher bulk modulus of HfO_2 indicates very stronger bonding between Hf and O in comparison with the bonding between Zr and O. This correlates with the observation that the Hf addition reduces the rate of Al_2O_3-scale growth more significantly than does Zr (as shown in Fig. 3).

The enthalpy of formation is related to the bond energy difference between the compounds and the constituent elements forming the compounds. For oxides, the enthalpy of formation can be expressed in terms of per mole of total atoms, per mole of metallic element, or per mole of oxygen. Assuming for simplicity that the outward diffusion of Al^{3+} in Al_2O_3 scale is through the exchange of cations via a vacancy mechanism, the enthalpy of formation can be expressed in terms of per mole of metallic element. Using the SGTE substance database [32], the enthalpies of formation ($\Delta_f H$) per mole of metallic atoms were calculated for HfO_2, ZrO_2, Y_2O_3, and Al_2O_3 and the results are shown in Table 1. The $\Delta_f H$ values for HfO_2, ZrO_2, and Y_2O_3 are 33%, 31%, and 14% more negative than that of Al_2O_3. It is thus inferred that more energy is needed in breaking Hf–O, Zr–O, and Y–O bonds than an Al-O bond, with Hf being the most effective followed by Zr and Y.

The bonding strength between a given cation and oxygen is also reflected by the melting temperature of the oxide. As shown in Table 1, HfO_2 has the highest melting temperature, followed by ZrO_2, Y_2O_3, and Al_2O_3, indicating that the strongest bonding is between Hf and oxygen, which in turn indicates that it is difficult for Al to break the Hf–O bonds in order to diffuse through the grain boundary. Using the SGTE substance database [32], the enthalpy of melting ($\Delta_m H$) can also be calculated. Since HfO_2, Zr_2O, and Y_2O_3 have several allotropic structures, the enthalpies of melting listed in Table 1 must consequently include the enthalpies of allotopic transitions and show that the values of HfO_2, ZrO_2, and Y_2O_3 are 127%, 101%, and 22% higher than that of Al_2O_3.

The bonding strength is also related to the cation-oxygen bond length. Terki et al. [33] calculated the inter-atomic distance between Hf–O and Zr–O bonds by

using first-principles calculations and compared the results with available experimental data [34, 35], showing that Hf–O (0.2204 nm) has shorter inter-atomic distance than Zr–O (0.2215 nm). The electron charge density between Hf and O was also calculated to be higher than that between Zr and O in their work. In addition, Milas et al. [25] calculated the bond lengths between adsorbed Hf or Y atoms and neighboring O atoms at an α-Al_2O_3 Σ11 $(10\bar{1}1)||(10\bar{1}\bar{1})$ grain boundary via first-principles calculations and compared the results with the experimental bond lengths in pure HfO_2 [36] and Y_2O_3 [37]. Their analysis showed that the Hf–O bond length (0.204–0.224 nm) is shorter than that of Y–O (0.229–0.237 nm). These results substantiated that the Hf–O bond is stronger than the Zr–O and Y–O bonds. The relatively strong RE–O bonding compared to Al–O would also affect the formation of both cation and oxygen vacancies. The stronger the bonding, the lower the probability for the RE–O bond to be broken. The correlation between bond strength and RE effectiveness in reducing Al_2O_3-scale growth is manifested in Figs. 1 and 3.

The effect of doping elements on bond strength in a high-angle grain boundary can be further correlated with theoretical calculations of adsorption energies. Hinnemann and Carter [38] studied the adsorption of Al, Hf, and Y on the α-Al_2O_3 (0001) surface using first-principles calculations. The adsorption energy of atom X (X = Al, Hf, Y) on the surface was calculated by

$$E_{\mathrm{ads},X} = E^{\mathrm{total}}_{X/\mathrm{Al_2O_3}} - \left(E^{\mathrm{total}}_{\mathrm{Al_2O_3}} + E^{\mathrm{total}}_{X}\right) \quad (1)$$

where $E^{\mathrm{total}}_{\mathrm{X/Al_2O_3}}$ is the total energy of the system with the atom X on the Al_2O_3 surface, $E^{\mathrm{total}}_{\mathrm{Al_2O_3}}$ the total energy of the pure α-Al_2O_3 with the surface, and E^{total}_{X} the total energy of the ground state of isolated atom X. The calculated adsorption energies are listed in Table 2. Hinnemann and Carter observed that Hf and Y bind to the same site as Al, but more strongly than Al on the α-Al_2O_3 (0001) surface and therefore effectively act as Al site blockers. These researchers also interpreted from their preliminary calculations that the chemistry of Zr on the α-Al_2O_3 (0001) surface was very similar to Hf and Y. Their calculations aligned with the experimental observations that Hf, Y, or Zr doping slows down the rate of Al_2O_3-scale growth [39].

Furthermore, Milas et al. [25] calculated the energetics of all possible adsorption sites for Al, O, Y, or Hf atoms at the α-Al_2O_3 Σ11 $((10\bar{1}1)||(10\bar{1}\bar{1})$ grain boundary through the first-principles calculations. They found that the adsorption sites for Al, Y, or Hf tend to be concentrated in similar regions of the grain boundary. The segregation of reactive elements to the grain boundaries may thus affect the accessibility of Al to those adsorption sites and slow down the Al diffusion and hence

Table 2 Calculated adsorption energies of Hf, Y and Al on α-Al_2O_3 (0001) by Hinnemann and Carter [38]

Elements	Adsorption energy (eV/atom)
Hf	−4.28
Y	−3.9
Al	−2.33

Al_2O_3-scale growth due to the stronger Hf–O, Y–O, and Zr–O bonding in comparison with Al-O bonding. These authors also compared the activation energies and pre-exponential factors for diffusion of Hf and Y on α-Al_2O_3 (0001) surface by using density functional theory and observed that the different bonding affects the activation energies rather than the pre-exponential factor in the Arrhenius equation for O diffusion. The calculated pre-exponential factors for Hf and Y were within an order of magnitude of one another, which indicates that the relative diffusion rate is governed by the energy barriers; Hf had a significantly higher activation barrier than Y in their work, which is aligned with the discussion of bonding strength in the present work.

Based on the bonding strength between the reactive element and oxygen, the addition of Zr is expected to be more effective than that of Y in reducing Al_2O_3-scale growth. However an experiment performed by Nychka and Clarke [40] showed the opposite behavior in that the addition of 0.1 wt% Y + 0.1 wt% Zr further decreases the oxide thickness to a greater extent than does the addition of only 0.1 wt% Zr in the FeCrAl alloys. They argued that Y blocks the outward diffusion of Al more than Zr does based on the larger ionic size of the former. However, as pointed out above, this cannot be the main reason because Y is less effective than Hf, with Hf and Zr having similar ionic sizes. Furthermore, the total amount of doped elements in 0.1 wt% Y + 0.1 wt% Zr is double than having only 0.1 wt% Zr, and the difference in the total doping concentration also affects the Al_2O_3-scale growth as discussed below.

Naumenko et al. [41] studied the effect of Y, Y + Hf, and Y + Zr additions on the oxide-scale microstructure by using TEM, showing that the scales on alloys doped with Y and Y + Hf exhibit a similar columnar grain morphologies, while doped with Zr, the Al_2O_3 microstructure in the inner part of the scale is different from the columnar morphology with considerable porosity, resulting in denser grain boundaries. As such, the Zr-doped scales may be expected to exhibit enhanced Al and O diffusion across the scale, giving higher Al_2O_3-scale growth rates.

Effect of Doping Level and Co-doping

In Fig. 1, 0.05% Y doping shows smaller weight changes than 0.1% Y. It can be understood from the published data that Y has a low solubility in alumina [42] and easily forms a ternary compound, YAG ($3Y_2O_3{\cdot}5Al_2O_3$), at low concentrations [43], resulting in an increase in total weight change measured. This suggests that the optimum doping level of Y is between 0.05 and 0.1%. On the other hand, the addition of 0.05% and 0.1% Hf shows similar weight changes, indicating that Hf may have saturated the grain boundaries, but its content in the substrate alloy is not high enough to form other oxides [44].

For alloys doped with more than one reactive element, it is important to compare with the same total amount of doping elements, such as 0.1% Y, 0.05% Y + 0.05% Hf, and 0.1% Hf. The effect of 0.05% Y + 0.05% Hf co-doping is better than that of 0.1% Y single doping because 0.1% Y is beyond the optimum level for Y. At the same time, 0.05% Y + 0.05% Hf co-doping is less effective than 0.1% Hf single doping, supporting that Hf plays a more important role than Y in reducing the rate

of Al_2O_3-scale growth. Furthermore, the co-doped alloys with 0.05% Hf + 0.05% Y and 0.1% Hf + 0.05% Y show less weight gain than that with 0.05% Y single doping due to both the higher total amount of doping and the greater effectiveness of Hf.

It is further noted that the weight changes of 0.05% Hf + 0.05% Y and 0.1% Hf + 0.05% Y after isothermal oxidation were similar since there is no significant difference between single doping of 0.05% Hf and 0.1% Hf. The weight change of the alloy with 0.1% Hf + 0.1% Y was similar to that of the alloy with 0.1% Y, indicating that the over-doped Y overshadows the benefit of Hf.

Summary

Through isothermal and thermal cyclic oxidation tests for Ni-base superalloys with or without reactive elements (Hf, Y or Zr) at 1150 °C, it is observed that the addition of reactive elements such as Hf, Y, or Zr to the alloys reduces the rate of Al_2O_3-scale growth, with Hf being the most effective. It is shown that the ionic size difference of reactive elements alone cannot explain their relative effectiveness. Based on the formation and melting enthalpies of oxides, cation-oxygen bond lengths, and adsorption energy calculations in the literature, the relative bonding strength between the cation and oxygen was utilized to understand the relative effectiveness of reactive elements in retarding the TGO growth. From the thermodynamic calculation, HfO_2 showed the highest enthalpy of formation and melting per mole of metallic atom followed by ZrO_2 and Y_2O_3, inferring that more energy is needed to break Hf–O bonds. The inter-atomic distance of Hf–O bond is also shorter than those of Zr–O and Y–O bonds, indicating the stronger bond of Hf–O and supporting the superior effect of Hf in reducing scale growth. In addition, the calculated adsorption energies, activation energies, and pre-exponential factors for diffusion of RE by using density functional theory in the literature are aligned with the discussion of bonding strength in the present work. In sum, the bonding strength between doped RE and oxygen plays a principal role in retarding the scale growth and must be one of the most important criteria to explain why Hf has the best effect.

Acknowledgements We are grateful to the Office of Naval Research (ONR) for support of this work under the contract number N0014-07-1-0638 and the Department of Energy (DOE) under grant number DE-FE0024056.

References

1. R. L. Jones, *Metallurgical and Ceramic Protective Coatings*, (Chapman and Hall, London, 1996), p. 194.
2. F. H. Stott and G. C. Wood, *Materials Science and Engineering* **87**, 267 (1987).
3. N. P. Padture, M. Gell and E. H. Jordan, *Science* **296**, 280 (2002).
4. P. Kofstad, *High Temperature Corrosion*, (Elsevier, London, 1988).
5. F. H. Stott, *Materials Science Forum* **251–254**, 19 (1997).
6. K. P. R. Reddy, J. L. Smialek and A. R. Cooper, *Oxidation of Metals* **17**, 429 (1982).
7. T. Amano, S. Yajima and Y. Saito, *Transactions of the Japan Institute of Metals* **20**, 431 (1979).
8. H. M. Hindam and W. W. Smeltzer, *Oxidation of Metals* **14**, 337 (1980).
9. R. Prescott, D. F. Mitchell, G. I. Sproule and M. J. Graham, *Solid State Ionics* **53–6**, 229 (1992).
10. B. A. Pint, J. R. Martin and L. W. Hobbs, *Oxidation of Metals* **39**, 167 (1993).

11. C. Mennicke, E. Schumann, M. Ruhle, R. J. Hussey, G. I. Sproule and M. J. Graham, *Oxidation of Metals* **49**, 455 (1998).
12. A. H. Heuer, *Journal of the European Ceramic Society* **28**, 1495 (2008).
13. A. H. Heuer and M. Zahiri Azar, *Scripta Materialia* **102**, 15 (2015).
14. A. H. Heuer, M. Zahiri Azar, H. Guhl, M. Foulkes, B. Gleeson, T. Nakagawa, Y. Ikuhara and M. W. Finnis, *Journal of the American Ceramic Society* **99**, 733 (2016).
15. S. Hayashi, T. Narita and B. Gleeson, *Materials Science Forum* **522–523**, 229 (2005).
16. W. C. Johnson, *Metallurgical Transactions A—Physical Metallurgy and Materials Science* **8**, 1413 (1977).
17. C. M. Wang, G. S. Cargill, M. P. Harmer, H. M. Chan and J. Cho, *Acta Materialia* **47**, 3411 (1999).
18. J. H. Cho, M. P. Harmer, H. M. Chan, J. M. Rickman and A. M. Thompson, *Journal of the American Ceramic Society* **80**, 1013 (1997).
19. J. Cho, H. M. Chan, M. P. Harmer and J. M. Rickman, *Journal of the American Ceramic Society* **81**, 3001 (1998).
20. T. Nakagawa, I. Sakaguchi, N. Shibata, K. Matsunaga, T. Mizoguchi, T. Yamamoto, H. Haneda and Y. Ikuhara, *Acta Materialia* **55**, 6627 (2007).
21. A. M. Huntz, *Materials Science and Engineering* **87**, 251 (1987).
22. K. Przybylski, *Journal of the Electrochemical Society* **134**, 469 (1987).
23. R. D. Shannon, *Acta Crystallographica Section A* **32**, 751 (1976).
24. C. M. Wang, G. S. Cargill, H. M. Chan and M. P. Harmer, *Interface Science* **8**, 243 (2000).
25. I. Milas, B. Hinnemann and E. A. Carter, *Journal of Materials Research* **23**, 1494 (2008).
26. R. D. Shannon and C. T. Prewitt, *Acta Crystallographica Section B-Structural Crystallography and Crystal Chemistry* **B 25**, 925 (1969).
27. A. H. Heuer, D. B. Hovis, J. L. Smialek and B. Gleeson, *Journal of the American Ceramic Society* **94**, 2698 (2011).
28. E. J. Kim and C. F. Chen, *Physics Letters A* **326**, 442 (2004).
29. M. Gaith and I. Alhayek, *Reviews on Advanced Materials Science* **21**, 183 (2009).
30. R. Sangiorgi, M. L. Muolo, D. Chatain and N. Eustathopoulos, *Journal of the American Ceramic Society* **71**, 742 (1988).
31. D. L. Anderson and O. L. Anderson, *Journal of Geophysical Research* **75**, 3494 (1970).
32. Scientific Group Thermodata Europe (SGTE), *Thermodynamic Properties of Inorganic Materials* (Springer, 1999).
33. R. Terki, H. Feraoun, G. Bertrand and H. Aourag, *Computational Materials Science* **33**, 44 (2005).
34. D. W. Stacy, D. R. Wilder and J. K. Johnston, *Journal of the American Ceramic Society* **55**, 482 (1972).
35. P. Aldebert and J. P. Traverse, *Journal of the American Ceramic Society* **68**, 34 (1985).
36. J. Adam and M. D. Rogers, *Acta Crystallographica* **12**, 951 (1959).
37. Y. Repelin, C. Proust, E. Husson and J. M. Beny, *Journal of Solid State Chemistry* **118**, 163 (1995).
38. B. Hinnemann and E. A. Carter, *Journal of Physical Chemistry C* **111**, 7105 (2007).
39. P. Y. Hou, *Journal of the American Ceramic Society* **86**, 660 (2003).
40. J. A. Nychka and D. R. Clarke, *Oxidation of Metals* **63**, 325 (2005).
41. D. Naumenko, V. Kochubey, L. Niewolak, A. Dymiati, J. Mayer, L. Singheiser and W. J. Quadakkers, *Journal of Materials Science* **43**, 4550 (2008).
42. J. D. Cawley and J. W. Halloran, *Journal of the American Ceramic Society* **69**, C195 (1986).
43. T. I. Mah and M. D. Petry, *Journal of the American Ceramic Society* **75**, 2006 (1992).
44. O. Fabrichnaya and C. Mercer, *Calphad-Computer Coupling of Phase Diagrams and Thermochemistry* **29**, 239 (2005).
45. L. Laversenne, C. Goutaudier, Y. Guyot, M. T. Cohen-Adad and G. Boulon, *Journal of Alloys and Compounds* **341**, 214 (2002).
46. K. Matsumoto, Y. Itoh and T. Kameda, *Science and Technology of Advanced Materials* **4**, 153 (2003).
47. J. E. Lowther, J. K. Dewhurst, J. M. Leger and J. Haines, *Physical Review B* **60**, 14485 (1999).
48. Y. N. Xu, Z. Q. Gu and W. Y. Ching, *Physical Review B* **56**, 14993 (1997).
49. S. Shang, Y. Wang and Z.-K. Liu, *Applied Physics Letters* **90**, 101909 (2007).